

## Temperature dependence of the free-exciton-emission linewidth in high-purity InP

R. Benzaquen

*Institute for Microstructural Sciences, National Research Council of Canada, Ottawa, Ontario, Canada K1A 0R6  
and Département de Physique et Groupe de Recherche en Physique et Technologie des Couches Minces, Université de Montréal,  
Case Postale 6128, Succursale Centre-Ville, Montréal, Québec, Canada H3C 3J7*

R. Leonelli

*Département de Physique et Groupe de Recherche en Physique et Technologie des Couches Minces, Université de Montréal,  
Case Postale 6128, Succursale Centre-Ville, Montréal, Québec, Canada H3C 3J7*

S. Charbonneau and P. J. Poole

*Institute for Microstructural Sciences, National Research Council of Canada, Ottawa, Ontario, Canada K1A 0R6*

A. P. Roth

*Institute for Microstructural Sciences, National Research Council of Canada, Ottawa, Ontario, Canada K1A 0R6  
and Département de Physique et Groupe de Recherche en Physique et Technologie des Couches Minces, Université de Montréal,  
Case Postale 62128, Succursale Centre-Ville, Montréal, Québec, Canada H3C 3J7*

(Received 24 May 1995)

Temperature-dependent photoluminescence measurements have been performed to study the linewidth of the  $n=1$  free-exciton transition in a high-purity  $n$ -type InP epilayer. The spectra reveal that the linewidth of the emission from upper-branch polaritons broadens rapidly when the temperature increases, while that of lower-branch polaritons narrows in the temperature range of 20–30 K. These results, which cannot be explained within the framework of the standard polariton transport model, are well reproduced by a phenomenological model that takes into account polariton scattering by bound excitons, ionized impurities, and phonons.

In direct-gap III-V semiconductors, exciton-photon interactions result in the formation of coupled modes called polaritons.<sup>1,2</sup> It is widely believed that polariton dynamics control the shape and lifetime of the free-exciton emission.<sup>3–5</sup> In particular, the low-temperature free-exciton photoluminescence (PL) of  $n$ -type GaAs with moderate donor concentration exhibits a dip at the energy corresponding to the exciton bottleneck, where the polariton group velocity is lowest. This dip, whose magnitude mostly depends on impurity concentration<sup>3,4</sup> and surface quality,<sup>6,7</sup> has been explained on the basis of polariton scattering by impurities or surface defects that prevent polaritons from reaching and escaping from the surface.<sup>3,4</sup> In samples with very low donor concentration ( $N_D \leq 10^{15} \text{ cm}^{-3}$ ), the dip disappears and the free-exciton-emission line shape becomes slightly asymmetrical, with a full width at half maximum (FWHM) of about 0.5 meV, both in GaAs (Refs. 3 and 7) and in InP.<sup>8</sup> Recently, however, free-exciton lifetime measurements<sup>7</sup> have cast some doubts on the use of the standard polariton transport model<sup>3,4</sup> to explain the kinetics of free-exciton recombination in direct-gap III-V semiconductors.

In order to examine this problem, we have investigated the free-exciton-emission linewidth as a function of temperature of a very-high-purity  $n$ -type InP epilayer grown by chemical beam epitaxy (CBE) on a (100) semi-insulating Fe-doped InP substrate.<sup>8</sup> The sample has a Hall mobility  $\mu_H$  of  $3.1 \times 10^5 \text{ cm}^2 \text{ V}^{-1} \text{ s}^{-1}$  at 50 K. The PL measurements were carried out in a liquid-helium flow cryostat with the sample mounted strain-free on a Cu block. The PL was excited using a HeNe laser, dispersed by a 0.64-m spectrom-

eter, and detected by a liquid-nitrogen-cooled charge-coupled device (CCD). The spectral resolution was set at 0.04 meV. We did not observe any variation of the free-exciton-emission linewidth for excitation power densities lower than  $1 \text{ W/cm}^2$ . This value was consequently used for all the temperature-dependent PL measurements.

Figure 1 displays the temperature dependence of the PL spectra in the excitonic region of our sample. For clarity all the spectra have been normalized to the same maximum value. At the lowest temperature, the PL spectrum is dominated by neutral shallow-donor-bound excitonic transitions ( $D_1^0, X$ )<sub>*n*</sub> (structures *d–g*), and by the lower polariton branch (LPB) of the  $n=1$  free-exciton (FE<sub>1</sub>) transition (structure *c*). We attribute the shoulder observed at higher photon energy to the upper polariton branch (UPB) of the FE<sub>1</sub> transition (structure *b*). In addition to the usual presence of shallow donors, a detailed electrical transport and optical study recently carried out on this sample indicated the presence of a broad band of localized deep-donor levels centered at 160 meV below the conduction-band edge with a FWHM of 165 meV.<sup>8</sup> Linked to the presence of this band, a bound excitonic PL band ( $D_2^0, X$ ) with a FWHM of  $\approx 22$  meV was observed below the acceptor-bound excitonic transition (structure *k* in the inset of Fig. 1).

The 4.2-K polariton emission line shape shown in Fig. 1 indicates a crystal with a low concentration of donors (see Table I). As displayed in Fig. 1, with increasing temperature, the PL intensity of the ( $D_1^0, X$ )<sub>*n*</sub> transitions are drastically reduced with respect to the PL intensity of the FE<sub>1</sub> transitions due to the thermal dissociation of the ( $D_1^0, X$ ) complex.

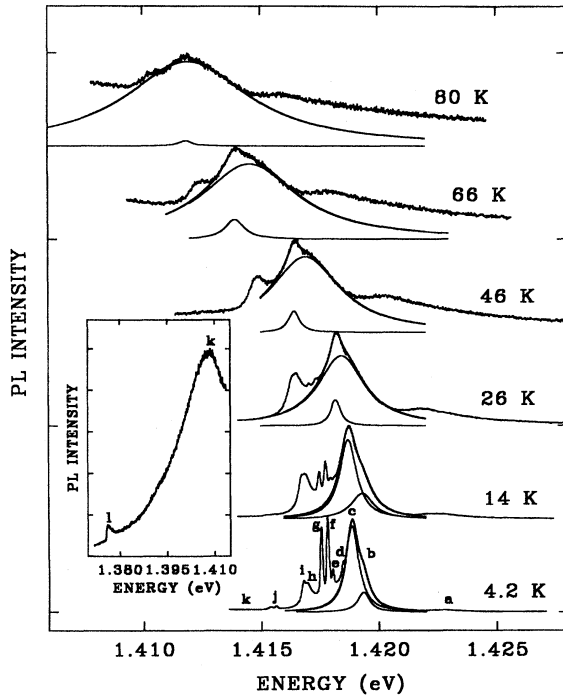


FIG. 1. Temperature-dependent PL spectra of  $n$ -type InP.  $a = \text{FE}_2$  is the  $n=2$  free-exciton transition.  $b$  and  $c$  are, respectively, the UPB and LPB parts of the  $\text{FE}_1$  transition;  $d-g$  are the neutral shallow-donor-bound excitonic transitions ( $D_1^0, X$ );  $h = (D_1^0, h)$  is the neutral shallow-donor to free-hole recombination;  $i = (D_1^+, X)$  is the ionized shallow-donor-bound excitonic transition;  $j = (A^0, X)$  is the neutral acceptor-bound excitonic transition;  $k = (D_2^0, X)$  is the neutral deep-donor-bound excitonic transition;  $l = (D_1^0, A^0)$  is the neutral shallow-donor-acceptor pair recombination. The solid curves are Lorentzian fits to structures  $b$  and  $c$ .

In contrast, the temperature dependence of the  $\text{FE}_1$  emission is quite intriguing. As the temperature is raised, the emission line shape can be seen as the sum of a narrow and a broad component. This is particularly evident in the spectrum taken at 46 K. To quantify this effect, we have empirically chosen a sum of two Lorentzians to take into account both the LPB and UPB emissions:

$$I(E) = \sum_{i=\text{LPB,UPB}} \frac{I_i}{1 + \left(\frac{E - E_{i,c}}{\gamma_i}\right)^2}, \quad (1)$$

TABLE I. Physical parameters of our InP sample.  $N_{D_1}$ ,  $N_{D_2}$ , and  $N_A$  are the shallow-donor, deep-donor, and acceptor concentrations, respectively;  $m^*$  and  $m_{\text{hh}}^*$  are, respectively, the electron and heavy-hole effective masses.  $E_{\text{LO}}$  is the longitudinal optical phonon energy.

$N_{D_1}^a$ ( $\text{cm}^{-3}$ )	$N_{D_2}^a$ ( $\text{cm}^{-3}$ )	$N_A^a$ ( $\text{cm}^{-3}$ )	$m^{*a}$ (a.u.)	$m_{\text{hh}}^{*b}$ (a.u.)	$E_{\text{LO}}^c$ (meV)
$7.9 \times 10^{13}$	$1.39 \times 10^{14}$	$3.7 \times 10^{13}$	0.082	0.85	42.8

<sup>a</sup>Reference 8.

<sup>b</sup>S. Adachi, J. Appl. Phys. **53**, 8775 (1982).

<sup>c</sup>Reference 10.

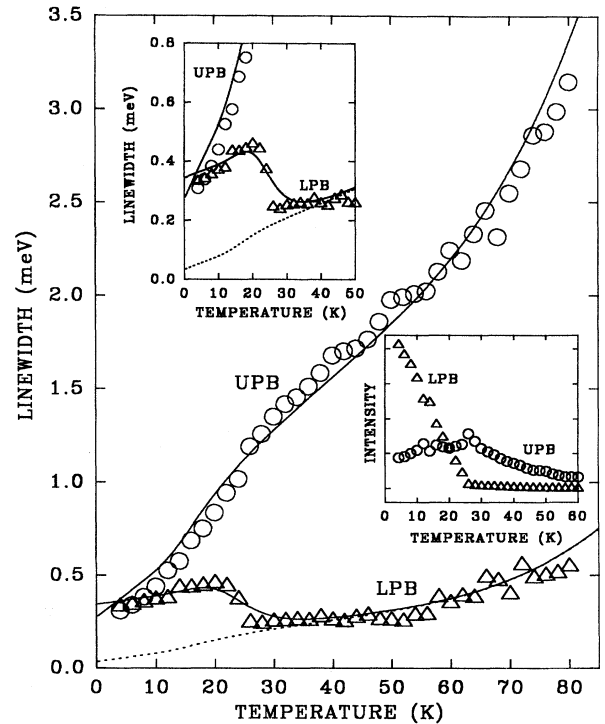


FIG. 2. Temperature dependence of the linewidth of the LPB (triangles) and UPB (circles) PL peaks of Fig. 1. The solid lines represent the full theoretical calculations obtained using Eq. (2) for the LPB and UPB, respectively. The dashed line is the theoretical calculation when deep-donor-bound exciton scattering is not included. The bottom right-hand inset displays the temperature dependence of the integrated PL intensities of structures  $b$  (circles) and  $c$  (triangles) of Fig. 1.

where the  $i$ th Lorentzian line shape of intensity  $I_i$  is centered at the photon energy  $E_{i,c}$ , with a linewidth  $\gamma_i$ . The results of an iterative least-squares fit to the normalized PL data using Eq. (1) are also shown in Fig. 1. The least-squares calculation has been carried out in an energy interval carefully chosen around  $E_{i,c}$  to minimize contributions from neighboring transitions to the overall line shape of the  $\text{FE}_1$  transition. The agreement between experimental and theoretical line shapes is excellent in the temperature range 4.2–80 K. We point out that the temperature dependencies of  $E_{\text{LPB},c}$  and  $E_{\text{UPB},c}$  are similar ( $E_{\text{LPB},c} < E_{\text{UPB},c}$  up to 80 K) and can be accurately described using the well-known Varshni equation.<sup>9</sup>

In Fig. 2, the experimental linewidths  $\gamma_i$  extracted from the fits are given as a function of temperature for both the LPB and UPB. As shown in Fig. 2,  $\gamma_{\text{UPB}}$  increases more rapidly with temperature than  $\gamma_{\text{LPB}}$ , which exhibits an initial increase followed by an abrupt decrease at  $\approx 25$  K. For sufficiently high temperatures, UPB emission can thus be observed in the same energy range as LPB emission. This observation is incompatible with the standard polariton transport model, which requires that the high-energy part of the  $\text{FE}_1$  emission be composed of upper-branch polaritons and the low-energy part of lower-branch polaritons, with some admixture of both types of polaritons in a narrow energy range near the longitudinal exciton energy  $E_L$ .<sup>4</sup> In the

bottom right-hand inset of Fig. 2, we display the temperature dependence of the integrated intensities  $I_{\text{LPB}}^*$  and  $I_{\text{UPB}}^*$ . At the lowest temperature, most of the polariton population resides in the bottleneck region of the LPB. As the temperature is raised to 25 K,  $I_{\text{LPB}}^*$  decreases very rapidly while  $I_{\text{UPB}}^*$  increases. This indicates that there exists an energy-transfer path whereby, for a given energy, the lower-branch polariton population is converted into upper-branch polaritons as the temperature is increased to 25 K.

In order to quantify our results, we have implemented the following phenomenological model. We assume that the temperature dependence of the linewidth  $\gamma_i$  of the FE<sub>1</sub> emission has the form<sup>10,11</sup>

$$\gamma_i(T) = \gamma_i + \gamma_{\text{BE}} + \gamma_A + \gamma_O. \quad (2)$$

The first term in Eq. (2),  $\gamma_i$ , arises from scattering due to impurities:

$$\gamma_i(T) = \sum_{i=1}^2 \gamma_{D_i^+} = \sum_{i=1}^2 \Gamma_{D_i^+} N_{D_i^+}, \quad (3)$$

where  $N_{D_i^+}$  is the concentration of ionized shallow ( $i=1$ ) or deep ( $i=2$ ) donors calculated following the procedure described in Ref. 8 and  $\Gamma_{D_i^+}$  is their associated broadening cross section, to be determined from our data analysis.

The second term in Eq. (2) is due to the scattering of polaritons by localized excitons. Such an interaction, which has recently been reported in GaAs/Ga<sub>x</sub>Al<sub>1-x</sub>As quantum wells,<sup>11</sup> is required to reproduce the observed net linewidth decrease of the LPB emission observed for temperatures in the range 20–30 K. The temperature dependence of  $\gamma_{\text{BE}}$  should be proportional to the density  $N_{\text{BE}}$  of bound excitons.<sup>12</sup>

$$\gamma_{\text{BE}}(T) = \gamma_{B,X} N_{\text{BE}} = \frac{\gamma_{B,X} N_{\text{pc}}}{2 + C_{B,X} T^{3/2} \exp\left[-\left(\frac{E_{B,X}}{k_B T}\right)\right]}, \quad (4)$$

$$C_{B,X} = \left(\frac{2\pi M k_B}{h^2 N_b^{2/3}}\right)^{3/2}, \quad (5)$$

where  $N_{\text{pc}} = 4 \times 10^{13} \text{ cm}^{-3}$  is the estimated density of photo-created electron-hole pairs,  $\gamma_{B,X}$  the bound exciton broadening cross section,  $E_{B,X}$  the localization energy of the bound excitons, and  $C_{B,X}$  a constant linked to the mass of the exciton  $M = m^* + m_{\text{hh}}^*$  and to the concentration of binding centers  $N_b$ . It is to be noted that  $\gamma_{B,X}$ ,  $E_{B,X}$ , and  $C_{B,X}$  can be determined independently from the other parameters by using the variation of  $\gamma_{\text{LPB}}$  in the temperature range 4.2–35 K.

The remaining terms in Eq. (2) are due to the interaction of excitons with the longitudinal-acoustical (LA) and longitudinal-optical (LO) phonon modes of the lattice and are given by<sup>10</sup>

$$\gamma_A(T) = \gamma_{\text{LA}} T, \quad (6)$$

TABLE II. Parameters extracted from the temperature dependence of the emission linewidth corresponding to the LPB and UPB of our sample.

	LPB	UPB
$\Gamma_{D_1^+}$ (meV cm <sup>3</sup> )	$1 \times 10^{-15}$	$6 \times 10^{-15}$
$\Gamma_{D_2^+}$ (meV cm <sup>3</sup> )	0	$2 \times 10^{-14}$
$\gamma_{\text{LA}}$ (meV K <sup>-1</sup> )	$4.5 \times 10^{-3}$	$2.5 \times 10^{-2}$
$\gamma_{\text{LO}}$ (meV)	100	350
$\gamma_{B,X}$ (meV cm <sup>3</sup> )	$1.55 \times 10^{-14}$	0
$C_{B,X}$ (K <sup>-3/2</sup> )	4.75	0
$E_{B,X}$ (meV)	12.4	0

$$\gamma_O(T) = \frac{\gamma_{\text{LO}}}{\exp\left(\frac{E_{\text{LO}}}{k_B T}\right) - 1}, \quad (7)$$

where  $\gamma_{\text{LA}}$  and  $\gamma_{\text{LO}}$  are, respectively, the LA coefficient and the LO linewidth parameter, to be determined from our data analysis, and  $E_{\text{LO}}$  is the LO phonon energy of InP.

The solid lines of Fig. 2 have been generated using Eq. (2) with the physical parameters of InP presented in Ref. 8. The results of the fits are reported in Table II. The overall agreement between the experimental data and the theoretical calculation is excellent in the temperature range 4.2–80 K. In particular, the model reproduces the observed net linewidth narrowing of the LPB. It is due to the vanishing of polariton scattering from  $(D_2^0, X)$  complexes as evidenced by the fitted value of  $E_{B,X}$  quoted in Table II. This value is close

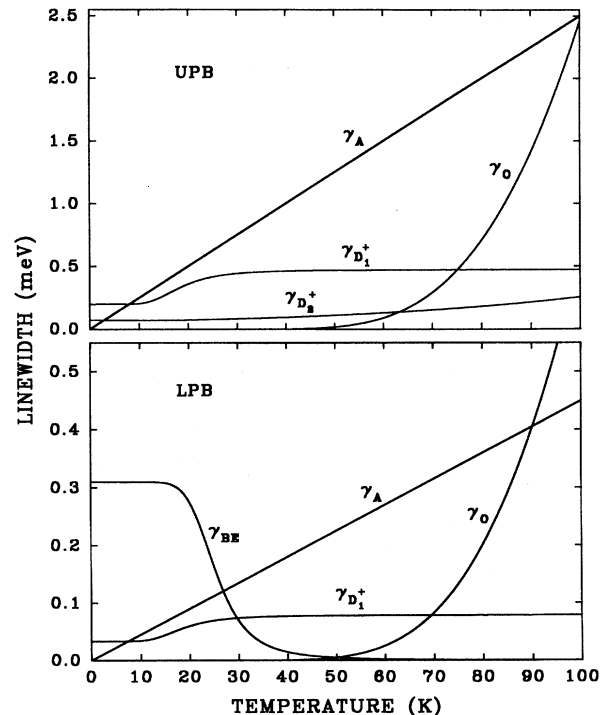


FIG. 3. Contributions to the linewidth of the PL of the LPB and UPB as a function of temperature.

to that obtained from the spectral position of the center of the  $(D_2^0, X)$  emission band (see inset of Fig. 1). Moreover, the value of  $C_{B,X}$  reported in Table II provides an estimate of the concentration of deep binding centers. Using the material parameters listed in Table II, we obtain  $N_b \approx 4 \times 10^{14} \text{ cm}^{-3}$ , a value close to that of  $N_{D_2}$  (see Table I).

Figure 3 summarizes the results of our model by showing the different contributions to  $\gamma_{\text{LPB}}$  and  $\gamma_{\text{UPB}}$ . The main contributions to  $\gamma_{\text{UPB}}$  come from  $\gamma_{D_1^+}$  and  $\gamma_A$  [ $\gamma_{D_2^+}$  contributes weakly to  $\gamma_{\text{LPB}}$  and  $\gamma_{\text{UPB}}$  since the deep centers are mostly neutral for temperatures below 80 K (Ref. 8)]. The temperature dependence of  $\gamma_{\text{LPB}}$  is strikingly different. For temperatures below  $\approx 25$  K,  $\gamma_{\text{BE}}$  dominates. Above  $\approx 20$  K, excitons dissociate from their deep binding centers and  $\gamma_{\text{BE}}$  decreases rapidly. For temperatures in the range 30–70 K,  $\gamma_{D_1^+}$  and  $\gamma_A$  are the main contributors to  $\gamma_{\text{LPB}}$ . However, the parameters  $\Gamma_{D_1^+}$  and  $\gamma_{\text{LA}}$  for the LPB are smaller by about a factor of 6 from those obtained for the UPB (see Table II). Above  $\approx 70$  K,  $\gamma_O$  contributes to both  $\gamma_{\text{UPB}}$  and  $\gamma_{\text{LPB}}$ , but the parameter  $\gamma_{\text{LO}}$  is smaller by about a factor of 3 for the LPB (see Table II).

As emphasized above, the coexistence of LPB and UPB emissions in the same energy range cannot be explained within the standard polariton transport model. This behavior can, however, be qualitatively reproduced by adding a phenomenological damping term to the polariton dispersion curve of InP.<sup>2</sup> This damping term does not affect significantly the LPB dispersion curve. However, it drastically changes the UPB dispersion curve, which then extends at energies below  $E_L$  and at wave vectors smaller than those of the LPB dispersion curve.<sup>2</sup> A density of states which spreads throughout the exciton resonance then becomes available to upper-branch polaritons. This modification of the usual polariton dispersion curves can also explain the different values of

$\gamma_{B,X}$  and  $\gamma_{D_1^+}$  obtained for the LPB and UPB. A bound exciton complex is characterized by a short-range scattering potential whereas, in a diluted system, an ionized impurity center is described by a long-range scattering potential. Polaritons with large wave vectors are thus more likely to interact with a short-range scattering potential and those with small wave vectors with a long-range one. Moreover, only lower-branch polaritons can have large wave vectors for energies above the transverse exciton energy.

In summary, we have presented a detailed temperature-dependent photoluminescence study of the  $n=1$  free-exciton transition in a high-purity, low-compensation,  $n$ -type InP epilayer. A Lorentzian line-shape analysis of the spectra reveals a process by which the lower-branch polariton population is converted into upper-branch polaritons as the temperature is increased to 25 K. We also find that the linewidth of the UPB emission increases more rapidly with temperature than that of the LPB so that, for high enough temperature, emissions from both polariton populations coexist in the same energy range. A phenomenological model that includes several scattering mechanisms was found to be in excellent agreement with the linewidth data extracted from the luminescence spectra in the temperature range 4.2–80 K. The model indicates that the scattering of upper-branch polaritons by ionized impurities and phonons is more efficient than that of lower-branch polaritons whereas deep-donor-bound excitons scatter lower-branch polaritons more efficiently than upper-branch ones. These results cannot be explained with the framework of the standard polariton transport model but can be qualitatively understood if a phenomenological damping factor is introduced in the polariton dispersion relation.

We thank M. W. C. Dharma-wardana for helpful comments on this manuscript and T. S. Rao for growing the InP sample.

<sup>1</sup>J. J. Hopfield, Phys. Rev. B **112**, 1555 (1958).

<sup>2</sup>C. Weisbuch and R. G. Ulbrich, in *Light Scattering in Solids*, edited by M. Cardona and G. Güntherodt (Springer-Verlag, Berlin, 1982), pp. 207–263.

<sup>3</sup>E. S. Koteles *et al.*, Phys. Rev. Lett. **55**, 867 (1985).

<sup>4</sup>T. Steiner *et al.*, Phys. Rev. B **34**, 1006 (1986).

<sup>5</sup>G. W. 't Hooft *et al.*, Phys. Rev. B **35**, 8281 (1987).

<sup>6</sup>T. Steiner *et al.*, Can. J. Phys. **67**, 242 (1989).

<sup>7</sup>D. J. Wolford *et al.*, in *Physics of Semiconductors: Proceedings of the XXI International Conference, Beijing, China, 1992*, ed-

ited by P. Jiang and H.-Z. Zheng (World Scientific, Singapore, 1993), p. 241.

<sup>8</sup>R. Benzaquen *et al.*, Phys. Rev. B **50**, 16 964 (1994).

<sup>9</sup>Y. P. Varshni, Physica **34**, 149 (1967).

<sup>10</sup>S. Rudin, T. L. Reinecke, and B. Segall, Phys. Rev. B **42**, 11 218 (1990).

<sup>11</sup>V. Srinivas, Y. J. Chen, and C. E. C. Wood, Solid State Commun. **89**, 611 (1994).

<sup>12</sup>R. Kubo, *Statistical Mechanics* (North-Holland, Amsterdam, 1965), p. 93.